PERGAMON

International Journal of Multiphase Flow 27 (2001) 657–671

International Journal of Multiphase Flow

www.elsevier.com/locate/ijmulflow

A delay theory for boiling flow stability analysis

D. Delmastro [a], L. Juanicó [b], A. Clausse [c,*]

[a] Comisión Nacional de Energía Atómica, 8400 Bariloche, Argentina

[b] CONICET and Comisión Nacional de Energía Atómica, 8400 Bariloche, Argentina

[c] Facultad de Ciencias Extractas, CNEA-CONICET and Universidad Nacional del Centro, 7000 Tandil, Argentina

Received 8 March 1999; received in revised form 11 June 2000

Abstract

An analysis of density-wave instabilities in boiling channels based on delay equations is presented. A two-dimensional mapping is derived from the flow conservation equations by assuming constant transport delays along the different parts of the channel. The simplicity of the final equation allows the fully analytical treatment of the system dynamics, both linear and non-linear, valid for high inlet subcoolings. Hopf bifurcations, subcritical and supercritical, could be identified and treated using perturbation methods. The derivation of a fully analytical criterion for Hopf bifurcation transcription was applied to determine the amplitude of limit cycles and the maximum allowed perturbations necessary to break the system stability.

Keywords: Instabilities; Boiling flow; Hopf bifurcations; Non-linear dynamics

1. Introduction

The phenomenon of density-wave instabilities in boiling channels has been extensively studied during the last 30 years (Lahey and Drew, 1980; Lahey, 1986). These oscillations may be encountered for certain operating conditions of boiling systems, where they become unstable due to lags in the phasing of the pressure-drop feedback mechanisms. Given the appropriate set of operating conditions, these delays may lead to self-excitation (Lahey and Moody, 1977). The most common manifestations of density-wave instabilities are self-sustained oscillations of the flow variables. The amplitudes of these oscillations can be very large, and can lead to flow reversals.

Density-wave instabilities in boiling systems, besides being scientifically interesting, represent serious practical implications for many industries. Phase-change heat exchangers, various

* Corresponding author.

E-mail address: clausse@exa.unicen.edu.ar (A. Clausse).

PII: S0301-9322(00)00039-2

chemical-process equipments and steam generators, to name a few, are potential candidates to experience density-wave instability.

The classical tool used to study the problem of density-wave instability in boiling systems is the linear frequency-domain analysis. Rather accurate and reliable models are now available for the analysis of complicated systems (Taleyarkhan et al., 1983; Peng et al., 1986; Xiao et al., 1993).

The study of the non-linear behavior of density-wave instabilities has attracted considerable interest recently (van Bragt et al., 1999). It has been found that Hopf bifurcations appear in boiling channels dynamics (Achard et al., 1985; Rizwan-Uddin and Dorning, 1988). Hopf-bifurcation theory (Hopf, 1942) shows the existence of periodic solutions in a narrow strip either on the stable side, or the unstable side, of a stability boundary. The case when the periodic solution lies on the stable side is called a subcritical bifurcation, and when it lies on the unstable side is called a supercritical bifurcation. When operating in the stable region, the theory shows that, for a subcritical case, sufficiently large perturbations will diverge from the steady state; while, in the supercritical case, all small but finite-amplitude perturbations decay to zero in the stable region. For operation in the unstable region in the subcritical case, all perturbations diverge from the equilibrium. In contrast, in the supercritical case, the periodic solution is stable in the region of linear instability, and thus all perturbations eventually evolve to a limit cycle.

In this paper, a theoretical analysis of a model of density-wave oscillations based on delay equations is presented. Non-linear effects are studied by means of Hopf bifurcation characterization, leading to the identification of metastable operating conditions, associated with subcritical bifurcations.

2. Boiling channel model

Let us consider the boiling channel shown in Fig. 1. The liquid enters at constant subcooled temperature and is heated uniformly along the channel. At certain location the fluid reaches its saturation temperature and starts to boil, exiting the channel as a two-phase mixture. In order to simplify the channel dynamics, the following assumptions are made:

- Equilibrium homogeneous model.
- The system pressure is constant.
- The heat flux is constant in space and time.
- Both phases are incompressible.
- Viscous dissipation and internal heat generation are neglected in the energy equation.
- Friction is concentrated at the inlet and the exit of the channel.

In the hypotheses above, the one-dimensional conservation equations of mass and energy yield to (Lahey and Moody, 1977)

$$u_e = u_i + \Omega(L_{ch} - \lambda), \tag{1}$$

where u_i and u_e are the inlet and exit velocities, L_{ch} the channel length, and the subcooled length, $\lambda(t)$, is defined by

$$\lambda(t) = \int_{t-\upsilon}^{t} u_i(t')\,dt'. \tag{2}$$

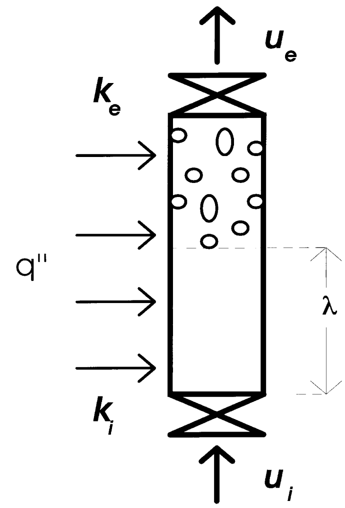

Fig. 1. Boiling channel.

In Eqs. (1) and (2), Ω is the characteristic frequency (qv_{fg}/h_{fg}), q the volumetric power, v_{fg} the specific volume difference, h_{fg} the latent heat of evaporation, and υ is the single-phase residence time.

For low frequencies Eq. (2) can be written as (Clausse et al., 1995)

$$\lambda(t) = \int_{t-\upsilon}^{t} u_i(t')\,dt' = v u_i(t - t_1), \tag{3}$$

where, t_1 is a time delay such that $0 < t_1 < v$.

Let us assume a quasi-static balance of forces in the momentum equation (Appendix C). At high Froude numbers the drag and acceleration forces then balance the external pressure head, that is,

$$(k_i - 1)\rho_f u_i^2 + (k_e + 1)\rho_e u_e^2 = \Delta p, \tag{4}$$

where k_i and k_e are the friction coefficients, ρ_f and ρ_e are the liquid and exit density, and Δp is the pressure drop.

Following a quasi-static approximation we can assume that the exit flow follows the history of the inlet flow (Clausse et al., 1995), that is,

$$\rho_e(t)u_e(t) = \rho_f u_i(t - t_2), \tag{5}$$

where t_2 is a certain transport delay.

In Appendices A and B, Eqs. (3) and (5) are analyzed in more detail, concluding that the best assessment for t_1 and t_2 is

$$t_2 = 2t_1 = v$$

and Eqs. (1)–(5) can be combined in a difference equation relating the shifted-time values of the inlet velocity $u = u_i(t)$, $u' = u_i(t - v/2)$, $u'' = u_i(t - v)$, according to

$$ku^2 + u''[u + N_{\rm sub}(1 - u')] = \frac{Eu}{k_{\rm e} + 1}, \tag{6}$$

where the velocity is expressed in units of $u_{\rm r} = v^{-1}L_{\rm ch}$. The reference velocity is chosen such that the boiling boundary is at the end of the channel when the dimensionless velocity is unity. The following dimensionless numbers were defined:

$N_{\rm sub} = \Omega v$, subcooling number,

$N_{\rm pch} = \Omega L_{\rm ch}/u_0$, phase-change number,

$k = (k_{\rm i} - 1)/(k_{\rm e} + 1)$, friction number,

$Eu = \Delta p/\rho_{\rm f} u_{\rm r}^2$, Euler number.

The operating conditions Eq. (6) is valid for are (Appendices A and B):

- $N_{\rm sub} \gg 1$ (values higher that 10 already yield good results),
- $N_{\rm sub}/N_{\rm pch} > 0.44$.

Eq. (6) represents an algebraic representation of the dynamics of a boiling channel by means of a two-dimensional mapping of the inlet velocity. Fig. 2 shows the evolution in the phase plane of a boiling channel according to Eq. (6). The theory compares fairly well with experiments provided that the friction terms dominate the flow dynamics (Juanico, 1997). Numerical analyses (in the time domain) performed in order to assess the matching of Eq. (6) with the complete differential model show good agreements for large $N_{\rm sub}$ (Clausse et al., 1995).

It should be stressed that Eq. (6) is only valid under some assumptions, namely:

- Constant and uniform heat flux.
- Friction concentrated at the inlet and the exit of the channel.
- Large subcooling numbers.
- Low Froude numbers.
- Low frequencies.

Examples of situations under which these assumptions are reasonable are short channels with small tube friction, and systems with strong pressure jumps at the inlet and outlet (orifices or valves).

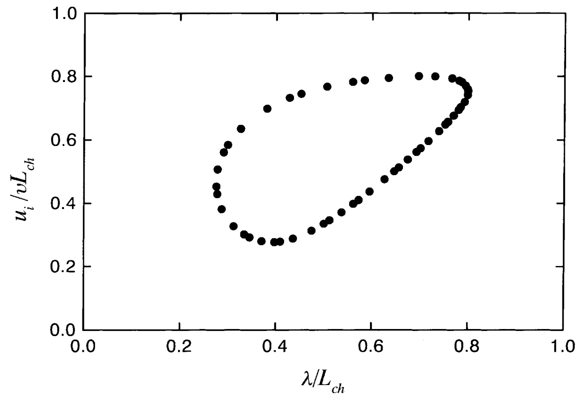

Fig. 2. Phase-plane dynamics of inlet velocity and subcooled length ($N_{\rm sub} = 50$, $N_{\rm pch} = 91.1$, $k = 19.5$).

3. Perturbation analysis

In the steady state (that is, $u = u' = u'' = u_0$) the inlet velocity should satisfy

$$ku_0^2 + u_0[u_0 + N_{\text{sub}}(1 - u_0)] = \frac{Eu}{(k_e + 1)}. \tag{7}$$

The value of the steady-state velocity, u_0, equals the steady-state subcooled fraction length $\lambda_0 = N_{\text{sub}}/N_{\text{pch}}$.

Linearizing Eq. (6) about u_0 leads to the linear difference equation

$$\{[u_0 + N_{\text{sub}}(u_0 - 1)]H^2 - N_{\text{sub}}u_0 H + (2k + 1)u_0\}(u - u_0) = 0, \tag{8}$$

where H is the shift operator (that is, $Hu(t) = u(t - \tau)$).

The steady state becomes oscillatory unstable when the module of any complex root of the characteristic equation associated to Eq. (8) becomes larger than unity, which occurs for (Clausse et al., 1995)

$$k = k_0 = \frac{N_{\text{sub}}(1 - u_0)}{2u_0}. \tag{9}$$

Thus, provided that the eigenvalues are complex and Eq. (9) is satisfied, the system dynamics is described by

$$u(t) = u_0 + \delta u \sin \omega t, \tag{10}$$

where δu is the perturbation amplitude, and the angular frequency ω is given by

$$\omega = \frac{\arctan(\beta/\alpha)}{\tau}, \tag{11}$$

where

$$\alpha = \frac{N_{\text{sub}}u_0}{2[u_0 + N_{\text{sub}}(1 - u_0)]}, \tag{12}$$

$$\beta = \sqrt{1 - \left[\frac{N_{\text{sub}}u_0}{u_0 + N_{\text{sub}}(1 - u_0)}\right]^2}. \tag{13}$$

The stability margin given by Eq. (9) was compared with the linear analysis of the distributed parameters model of density-waves (Achard et al., 1985; Lahey, 1986), showing excellent agreement for subcooling numbers higher than 10. Fig. 3 shows the comparison between stability margins calculated using different degrees of simplification.

Following the standard procedure in Hopf bifurcation theory (Hassard et al., 1981; Hale and Kokak, 1991), let us consider a small departure of k from k_0. The system variables can be expanded in powers of a small parameter ε according to

$$u(t) = u_0 + \varepsilon u_1(t) + \varepsilon^2 u_2(t) + \cdots, \tag{14a}$$

$$k = k_0 + k_1\varepsilon + k_2\varepsilon^2 + \cdots, \tag{14b}$$

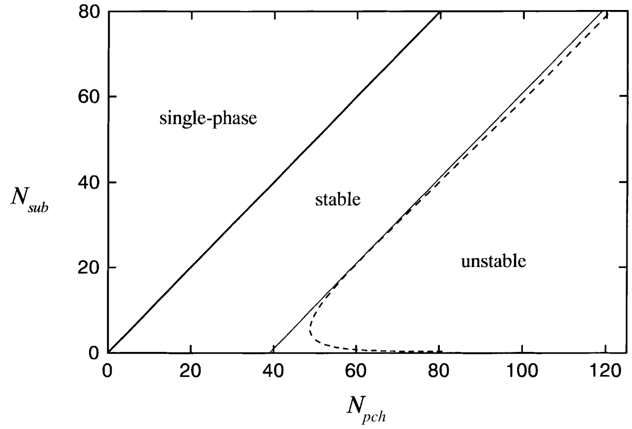

Fig. 3. Linear stability margin ($k = 19.5$). Present model (solid line), distributed parameter model (dashed line).

$$t = \theta\left(\frac{1}{\omega} + \tau_1\varepsilon + \tau_2\varepsilon^2 + \cdots\right). \tag{14c}$$

The time stretching defined in Eq. (14c) implies over the delays:

$$u(t-\tau) = u(\theta - \omega\tau) + \left(\tau_1\varepsilon + \tau_2\varepsilon^2 + \cdots\right)\frac{\partial u(\theta')}{\partial\theta'}\bigg|_{\theta'=\theta-\omega\tau} + \frac{1}{2}\left(\tau_1\varepsilon + \tau_2\varepsilon^2 + \cdots\right)^2\frac{\partial^2 u(\theta')}{\partial\theta'^2}\bigg|_{\theta'=\theta-\omega\tau} + \cdots \tag{15}$$

and a similar expression for $u(t - 2\tau)$.

Combining Eqs. (6), (14a)–(15) and collecting like powers of ε yields to

$$\left\{[u_0 + N_{\mathrm{sub}}(u_0 - 1)]H^2 - N_{\mathrm{sub}}u_0H + (2k+1)u_0\right\}u_n = S_n, \tag{16}$$

where

$$S_1 = 0, \tag{17a}$$

$$S_2 = -k_0u_1^2 - 2u_0k_1u_1 + u_0\tau_1\left(N_{\mathrm{sub}}\frac{\mathrm{d}u_1'}{\mathrm{d}\theta} - \frac{\mathrm{d}u_1''}{\mathrm{d}\theta}\right) - u_1u_1'' + N_{\mathrm{sub}}u_1'u_1'', \tag{17b}$$

$$\begin{aligned} S_3 = {} & -2k_0u_1u_2 - 2u_0k_2u_1 - k_1\left(2u_0u_2 + u_1^2\right) - u_0\left(\frac{\mathrm{d}u_1''}{\mathrm{d}\theta}\tau_2 + \frac{\mathrm{d}^2u_1''}{\mathrm{d}\theta^2}\tau_1^2 + \frac{\mathrm{d}u_2''}{\mathrm{d}\theta}\tau_1\right) - u_1''u_2 \\ & - u_1\left(\frac{\mathrm{d}u_1''}{\mathrm{d}\theta}\tau_1 + u_2''\right) + N_{\mathrm{sub}}u_0\left(\frac{\mathrm{d}u_1'}{\mathrm{d}\theta}\tau_2 + \frac{\mathrm{d}u_2'}{\mathrm{d}\theta}\tau_1 + \frac{\mathrm{d}^2u_1'}{\mathrm{d}\theta^2}\tau_1^2\right) + N_{\mathrm{sub}}u_1''\left(\frac{\mathrm{d}u_1'}{\mathrm{d}\theta}\tau_1 + u_2'\right) \\ & + N_{\mathrm{sub}}u_1'\left(\frac{\mathrm{d}u_1''}{\mathrm{d}\theta}\tau_1 + u_2''\right) - N_{\mathrm{sub}}(1-u_0)\left(\frac{\mathrm{d}u_1''}{\mathrm{d}\theta}\tau_2 + \frac{P\mathrm{d}^2u_1''}{\mathrm{d}\theta^2}\tau_1^2 + \frac{\mathrm{d}u_2''}{\mathrm{d}\theta}\tau_1\right). \end{aligned} \tag{17c}$$

Under the proper circumstances (that is, complex eigenvalues crossing the imaginary axis as the parameter k is varied) the Hopf theorem states that a family of periodic solutions, with small amplitude ε, exists in the neighborhood of the stability boundary. The necessary and sufficient condition for Eqs. (17a)–(17c) to have a periodic solution is the so-called "Fredholm alternative" condition (Achard et al., 1985; Lahey, 1986):

$$\frac{1}{\pi}\int_0^{2\pi} S_n\,\mathrm{e}^{-\mathrm{j}\theta}\,\mathrm{d}\theta = 1. \tag{18}$$

Let us introduce the following solutions for Eq. (16):

$$u_1 = \cos\theta, \tag{19a}$$

$$u_2 = a + b_1\cos\theta + b_2\sin\theta + c_1\cos 2\theta + c_2\sin 2\theta. \tag{19b}$$

Now, combining Eqs. (16)–(19b) yields to:

$$k_1 = 0, \tag{20a}$$

$$\tau_1 = 0, \tag{20b}$$

$$b_1 = 0, \tag{20c}$$

$$b_2 = 0, \tag{20d}$$

$$a = \frac{1}{4}\,\frac{N_{\mathrm{sub}}\left(\frac{u_0-1}{u_0}\right) + \cos(2\omega\tau) - N_{\mathrm{sub}}\cos(\omega\tau)}{2(N_{\mathrm{sub}}+u_0) - 3N_{\mathrm{sub}}u_0}, \tag{21}$$

$$c = c_1 + \mathrm{i}c_2 = \frac{1}{4}\left[\frac{\left(\frac{N_{\mathrm{sub}}(1-u_0)}{u_0}\right)\mathrm{e}^{2\omega\tau\mathrm{i}} + 1 - N_{\mathrm{sub}}\,\mathrm{e}^{-2\omega\tau\mathrm{i}}}{N_{\mathrm{sub}}u_0 - 2(u_0 + N_{\mathrm{sub}}(1-u_0))\cos(2\omega\tau)}\right], \tag{22}$$

$$\begin{aligned}
2u_0k_2 = {} & -\frac{N_{\mathrm{sub}}(1-u_0)}{u_0}(a+c_1) - c_1\left(\alpha^4 - 6\alpha^2\beta^2 + \beta^4\right) - a + 4c_2\left(\alpha^3\beta - \alpha\beta^3\right)\\
& + N_{\mathrm{sub}}a\left(\alpha^2-\beta^2\right) + N_{\mathrm{sub}}(c_1 + a\alpha) + N_{\mathrm{sub}}c_1\left(\alpha^3 - 3\alpha\beta^2\right) - N_{\mathrm{sub}}c_2\left(3\alpha^2\beta - \beta^3\right)\\
& - (a+c_1)\left(\alpha^2-\beta^2\right) - 2c_2\alpha\beta - \beta\{N_{\mathrm{sub}}u_0 - 4\alpha[u_0 + N_{\mathrm{sub}}(1-u_0)]\}\\
& \times\left[N_{\mathrm{sub}}c_2(1-u_0)/u_0 - N_{\mathrm{sub}}c_2 - N_{\mathrm{sub}}c_1\left(3\alpha^2\beta - \beta^3\right) - 2aN_{\mathrm{sub}}\alpha\beta + c_2\left(\alpha^4 - 6\alpha^2\beta^2 + \beta^4\right)\right.\\
& \left. + 4c_1\left(\alpha^3\beta - \alpha\beta^3\right) - aN_{\mathrm{sub}} - N_{\mathrm{sub}}c_2\left(\alpha^3 - 3\alpha\beta^2\right) + 2(a-c_1)\alpha\beta + c_2\left(\alpha^2-\beta^2\right)\right]\\
& \div\left\{N_{\mathrm{sub}}u_0\alpha - [u_0 + N_{\mathrm{sub}}(1-u_0)]2\left(\alpha^2-\beta^2\right)\right\},
\end{aligned} \tag{23}$$

$$\begin{aligned}
\tau_2\tau\omega^2 = {} & \left[c_2N_{\mathrm{sub}}(1-u_0)/u_0 - 4c_1\left(\alpha^3\beta - \alpha\beta^3\right) + c_2\left(\alpha^4 - 6\alpha^2\beta^2 + \beta^4\right) + 2N_{\mathrm{sub}}a\alpha\beta\right.\\
& + N_{\mathrm{sub}}a\beta + N_{\mathrm{sub}}c_1\left(3\alpha^2\beta - \beta^3\right) - N_{\mathrm{sub}}c_2\left(\alpha^3 - 3\alpha\beta^2\right) - N_{\mathrm{sub}}c_2 - 2a\alpha\beta + 2c_1\alpha\beta\\
& \left. + c_2\left(\alpha^2-\beta^2\right)\right] \div \left\{N_{\mathrm{sub}}u_0\alpha - 2\left(\alpha^2-\beta^2\right)[u_0 + N_{\mathrm{sub}}(1-u_0)]\right\}.
\end{aligned} \tag{24}$$

4. Discussion of results

Eq. (23) constitutes an important result concerning the non-linear properties of boiling channel dynamics. In first place, the sign of k_2 determines the character of the bifurcation, that is:

$k_2 > 0 \Rightarrow$ subcritical bifurcation;

$k_2 < 0 \Rightarrow$ supercritical bifurcation.

Under subcritical conditions, the system is unstable for excitations of any amplitude in the linear instability region. Moreover, it is also unstable within some region of linear stability for large enough amplitude excitations. On the other hand, a supercritical system exhibits bounded periodic solutions (limit cycles) in some region of linear instability (Lahey, 1986). The singular condition for which $k_2 = 0$, represents the transcritical point where the system switches from subcritical to supercritical. Fig. 4 shows this condition in the parameter plane (N_{sub}, u_0). It can be seen that for large subcooling numbers the character of the bifurcation is determined only by the value of u_0.

Eq. (23) can also be applied to calculate the amplitude of the limit cycles (when supercritical bifurcations occur) or alternatively the size of the minimum perturbation that triggers instabilities within the linear stable domain (when subcritical bifurcations occur). In effect, taking only the lower-order terms, Eqs. (14a)–(14c) leads to

$$k = k_0 + k_2\varepsilon^2, \tag{25}$$

$$u = u_0 + \varepsilon \cos \omega t. \tag{26}$$

Thus, the relative amplitude of the perturbation can be related with the departure of k from the linear limit, k_0, that is,

$$\left(\frac{\varepsilon}{u_0}\right)^2 = \frac{k_0}{k_2 u_0^2}\left(\frac{k - k_0}{k_0}\right). \tag{27}$$

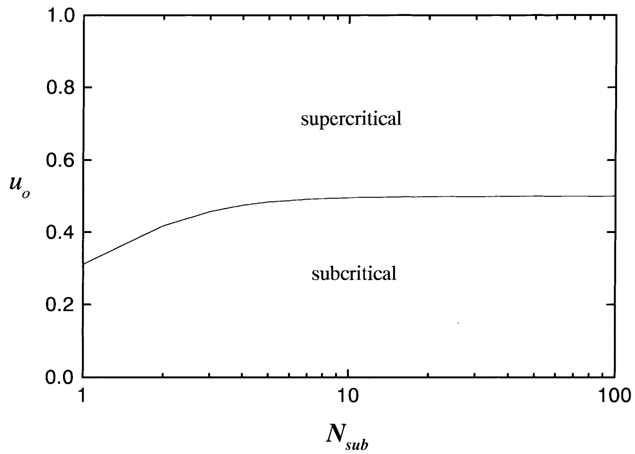

Fig. 4. Transcritical map ($k_2 = 0$).

For subcritical bifurcations ($k_2 > 0$), the lower the value of the factor $k_0/(k_2 u_0^2)$, the lower is the perturbation required to destabilize a linearly stable condition. Therefore, in stable regions where this coefficient is low, a special attention should be given to the response of the system to finite-amplitude perturbations. On the other hand, for supercritical bifurcations ($k_2 < 0$), the higher the value of $k_0/(k_2 u_0^2)$, the smaller is the amplitude of the limit cycles. Therefore, in unstable regions where $k_0/(k_2 u_0^2)$ is high, the response of the system could be acceptable for design, for the oscillations might remain within controllable ranges. Taking into account these effects of the coefficient $k_0/(k_2 u_0^2)$ on the stability of the boiling channel, a risk indicator function can be constructed, which quantifies the potential danger of linearly stable operating conditions, which actually can become unstable under finite perturbations (metastability):

$$R = \exp\left[\frac{k_0}{k_2 u_0^2}\right]. \tag{28}$$

Higher R implies more dangerous situations (metastable regions or large amplitude limit cycles), and R vanishes in the less risky situations (stable under large perturbations or small amplitude limit cycles). Values of R larger than 1 indicate potential metastable conditions. For larger N_{sub}, R depends only on u_0. This limit is depicted in Fig. 5. The transcription ($R = 1$) is located at $u_0 = 0.5$. For values of u_0 larger than 0.5, R decreases substantially, which means that stable limit cycles of small amplitude are expected close to the instability boundary. Fig. 6 shows the contour map of R in the plane (N_{pch}, N_{sub}) which are the classical parameters used in linear stability plots of boiling channels. The map of R can be applied as a warning indicator in those linearly stable regions where metastability is likely to occur.

The discussion of Eqs. (20b) and (24) is also interesting. These equations give information about the frequency of the oscillations. From Eq. (14c), the second-order frequency correction is given by

$$\omega(\varepsilon) = \frac{\omega}{1 + \omega\tau_2\varepsilon^2}, \tag{29}$$

where τ_2 is related to N_{sub} and u_0 through Eq. (24). The change in the period of the oscillation, T, is given by

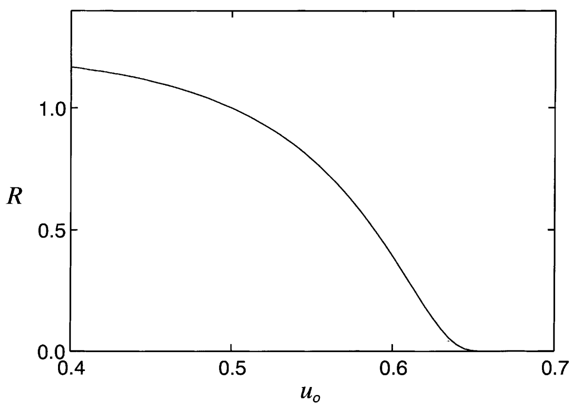

Fig. 5. Risk indicator for large N_{sub}.

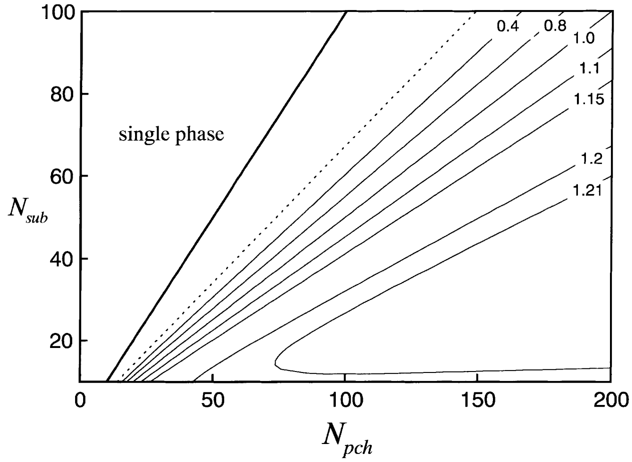

Fig. 6. Contour map of the risk indicator.

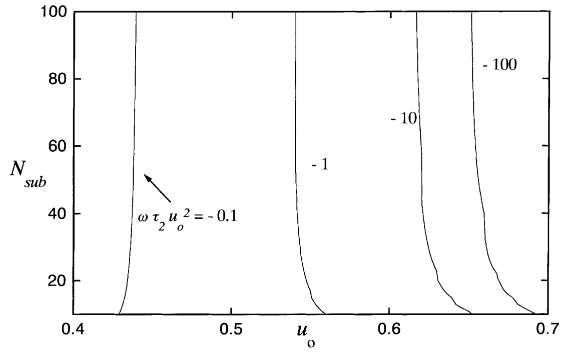

Fig. 7. Contour map of the frequency coefficient, $\omega\tau_2 u_0^2$.

$$\frac{\Delta T}{T} = \omega\tau_2 u_0^2 \left(\frac{\varepsilon}{u_0}\right)^2. \tag{30}$$

Fig. 7 shows the contour map of the coefficient $\omega\tau_2 u_0^2$. It can be seen that the coefficient $\omega\tau_2 u_0^2$ is always negative, which means that the oscillation period decreases as amplitude increases. For large N_{sub}, $\omega\tau_2 u_0^2$ depends only on u_0. This limit is shown in Fig. 8. The value of the coefficient $\omega\tau_2 u_0^2$ decreases abruptly for u_0 larger than 0.5, meaning that the oscillation period is very sensitive at higher u_0.

Finally, Eqs. (1) and (21) can be combined to calculate the bias of the average inlet velocity due to non-linear effects, which is given by

$$\frac{\bar{u} - u_0}{u_0} = a u_0 \left(\frac{\varepsilon}{u_0}\right)^2. \tag{32}$$

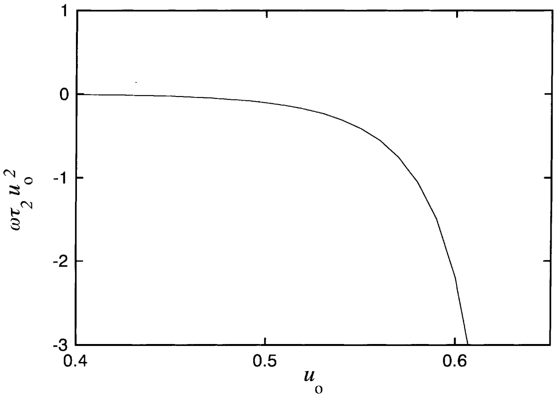

Fig. 8. Limit of the frequency coefficient for large N_{sub}.

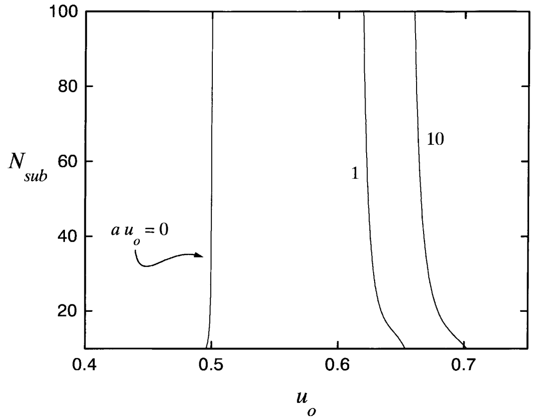

Fig. 9. Contour map of the bias coefficient, au_0.

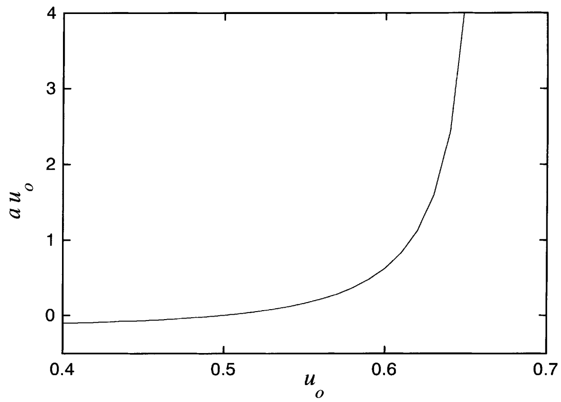

Fig. 10. Limit of the bias coefficient for large N_{sub}.

Eq. (32) indicates that the average value of the inlet velocity, $\bar{u}$, does not coincide with the steady-state value that balances the momentum equation, u_0, and consequently care should be taken in analyzing experimental data obtained in oscillating flows. Fig. 9 shows the contour map of the bias coefficient, au_0, and the limit for large N_{sub} is plotted in Fig. 10. It can be observed that the bias is always positive for supercritical bifurcations, meaning that the average velocity is larger than the steady-state value.

5. Conclusions

A mathematical model of boiling channels dynamics based on delay equations was derived from the homogeneous two-phase flow conservation equations. A two-dimensional mapping results from the assumption of constant transport delays along the channel. The stability of the discrete dynamics was analyzed using linear perturbations about the steady state, showing good agreement with more sophisticated models.

The character of the oscillatory instabilities was studied using Hopf perturbation methods. The analysis leads to the identification of subcritical and supercritical bifurcations. It was possible to characterize the non-linear behavior of the system using a "risk" function, which provides a measure of the amplitude of the limit cycles (either stable or unstable). Moreover, the analysis permits the characterization of the non-linear effects in the period of oscillation and the bias of the average inlet velocity. The theoretical results derived using the present approach will be very useful for contrasting against experimental data, and will serve as a guidance procedure in future non-linear analyses of more complex boiling channel models.

Appendix A. Relation between $u_i(t)$ and $\lambda(t)$

Let us consider a harmonic perturbation of the inlet velocity, u_i:

$$u_i(t) = u_0 + \delta u \sin \omega t. \tag{A.1}$$

The subcooled length, λ, responds following Eq. (2), which gives

$$\lambda(t) = \int_{t-\upsilon}^{t} u_i(t')\,\mathrm{d}t' = v u_0 + \frac{\delta u}{\omega}[\cos \omega(t - v) - \cos \omega t]. \tag{A.2}$$

Regarding that

$$\cos \omega t = \cos \omega\left(t - \frac{v}{2} + \frac{v}{2}\right) = \cos \omega\left(t - \frac{v}{2}\right) \cos \frac{\omega v}{2} - \sin \omega\left(t - \frac{v}{2}\right) \sin \frac{\omega v}{2}, \tag{A.3}$$

$$\cos \omega(t - v) = \cos \omega\left(t - \frac{v}{2} - \frac{v}{2}\right) = \cos \omega\left(t - \frac{v}{2}\right) \cos \frac{\omega v}{2} + \sin \omega\left(t - \frac{v}{2}\right) \sin \frac{\omega v}{2}. \tag{A.4}$$

Eq. (A.2) can be written as

$$\lambda(t) = vu_0 + \frac{2\delta u}{\omega} \sin \frac{\omega v}{2} \sin \omega\left(t - \frac{v}{2}\right)$$
$$= vu_{\mathrm{i}}\left(t - \frac{v}{2}\right)\left(\frac{2}{\omega v} \sin \frac{\omega v}{2}\right) + vu_0\left(1 - \frac{2}{\omega v} \sin \frac{\omega v}{2}\right). \tag{A.5}$$

For $\omega v/2 < 1$,

$$\frac{2}{\omega v} \sin \frac{\omega v}{2} < 0.017.$$

Also,

$$\lambda(t) \cong vu_{\mathrm{i}}\left(t - \frac{v}{2}\right). \tag{A.6}$$

By comparing Eqs. (3) and (A.6) one concludes that the approximation given by Eq. (3) is valid considering $t_1 = v/2$. In such case, the angular frequency can be calculated using Eq. (11), which for $N_{\mathrm{sub}} \gg 1$ gives

$$\frac{\omega v}{2} = \arctan\left(2\sqrt{\left(\frac{1-u_0}{u_0}\right)^2 - 1}\right). \tag{A.7}$$

Therefore, the approximate Eq. (3) is valid for

$$u_0 > \frac{1}{1 + \sqrt{1 + \frac{\tan^2(1)}{4}}} = 0.44. \tag{A.8}$$

Appendix B. Relation between $\rho_{\mathrm{e}}u_{\mathrm{e}}$ and u_{i}

The density and the velocity at the channel exit, $\rho_{\mathrm{e}}(t)$ and $u_{\mathrm{e}}(t)$, the inlet velocity, $u_{\mathrm{i}}(t)$, can be exactly written in terms of the subcooled length, $\lambda(t)$ (Achard et al., 1985):

$$\rho_{\mathrm{e}} = \mathrm{e}^{-\theta N_{\mathrm{sub}}}, \tag{B.1}$$

$$1 - \lambda(t) = \int_0^{\theta} u_{\mathrm{i}}(t - 1 - t')\, \mathrm{e}^{t' N_{\mathrm{sub}}}\, \mathrm{d}t', \tag{B.2}$$

$$u_{\mathrm{e}}(t) = u_{\mathrm{i}}(t) + N_{\mathrm{sub}}[1 - \lambda(t)], \tag{B.3}$$

where v is used as reference time.

The order of magnitude of θ can be estimated using the steady-state values in Eq. (B.2), which gives

$$\theta = \frac{\ln(N_{\mathrm{pch}} - N_{\mathrm{sub}} + 1)}{N_{\mathrm{sub}}}. \tag{B.4}$$

Therefore, for large $N_{\rm sub}$, θ vanishes. This result is in agreement with the calculations of Rizwan-Uddin (1994) from experimental data showing that the two-phase residence time is much shorter than the single-phase delay. In such case, Eq. (B.2) can be approximated by

$$1-\lambda(t)=\frac{u_{\rm i}(t-1)(e^{\theta N_{\rm sub}}-1)}{N_{\rm sub}}. \tag{B.5}$$

Combining Eqs. (B.1) and (B.3) and (B.5) gives

$$\rho_{\rm e}(t)u_{\rm e}(t)=u_{\rm i}(t-1)\left\{\frac{u_{\rm i}(t)+N_{\rm sub}[1-\lambda(t)]}{u_{\rm i}(t-1)+N_{\rm sub}[1-\lambda(t)]}\right\}. \tag{B.6}$$

For large $N_{\rm sub}$

$$\rho_{\rm e}(t)u_{\rm e}(t)=u_{\rm i}(t-1). \tag{B.7}$$

Comparing Eqs. (B.7) and (5), one concludes that $t_2=1$ (in units of v), and since $t_1=v/2$,

$$t_2=\frac{t_1}{2}.$$

Appendix C. Quasi-static momentum equation

Assuming the homogenous two-phase flow model, the one-dimensional momentum balance is written as

$$\frac{\partial\rho u}{\partial t}+\frac{\partial\rho u^2}{\partial z}+g\rho+f\rho u^2=\frac{\partial p}{\partial z}, \tag{C.1}$$

where the different terms in the right-hand side represent the pressure drops due to inertia, acceleration, gravity and friction, and the left-hand side is the local pressure gradient.

The quasi-static approximation states that the inertia term is small compared to the other pressure drops, which is valid for low frequencies:

$$\frac{\partial\rho u^2}{\partial z}+g\rho+f\rho u^2=\frac{\partial p}{\partial z}, \tag{C.2}$$

where g is the gravity, p the pressure, and f is the friction coefficient.

Integrating Eq. (C.2) along a boiling channel subject to constant pressure drop boundary conditions leads to

$$\rho_{\rm e}u_{\rm e}^2-\rho_{\rm f}u_{\rm i}^2+g\int_0^{L_{\rm ch}}\rho\,{\rm d}z+\int_0^{L_{\rm ch}}f\rho u^2\,{\rm d}z=\Delta p. \tag{C.3}$$

Assuming that the frictions at the inlet and exit are much larger than the friction along the channel (that is, valves, restrictions, orifices):

$$f=k_{\rm i}\delta(z)+k_{\rm e}\delta(z-L_{\rm ch}), \tag{C.4}$$

where $\delta(z)$ represents the Dirac delta.

Replacing Eq. (C.4) in (C.3) gives

$$(k_i - 1)\rho_f u_i^2 + (k_e + 1)\rho_e u_e^2 + \frac{\rho_f u_0^2}{Fr}\int_0^{L_{ch}} \rho \, dz + = \Delta p, \tag{C.5}$$

where the Froude number is defined as

$$Fr = \frac{\rho_f u_0^2}{g}. \tag{C.6}$$

At high Froude numbers (horizontal channels or high friction flows) the gravity term is small, yielding to Eq. (4).

References

Achard, J.L., Drew, D.A., Lahey, R.T., 1985. The analysis of non-linear density-wave oscillations in boiling channels. J. Fluid Mech. 155, 213–232.

van Bragt, D.D.B., Rizwan-Uddin, van Der Hagen, T.H.J., 1999. Nonlinear analysis of a natural circulation boiling water reactor. Nucl. Sci. Eng. 13, 23–44.

Clausse, A., Delmastro, D., Juanico, L. 1995. A simple delay model for the dynamics of boiling channels. In: NURETH-7 Conference, NUREG-CP-0142, vol. 4, Saratoga Springs, USA, pp. 3232–3244.

Hale, J., Kokac, H., 1991. Dynamics and Bifurcations. Springer, New York.

Hassard, B.D., Kazarinoff, N.D., Wan, Y.H., 1981. Theory and Application of Hopf Bifurcation. London Mathematical Society Lecture Notes, Series 41, Cambridge University, Cambridge.

Hopf, E., 1942. Abzweigung einer periodischen Losung von einer stationaren Losung eines Differentialsystems. Ber. Math. Phys. Classe Sachs. Acad. Bis. Leipzig 94, 1–22.

Juanico, L., 1997. Identification of dynamical basins in boiling flows. Ph.D. Thesis, Instituto Balseiro, Argentina.

Lahey, R.T., 1986. Advances in the analytical modeling of linear and non-linear density-wave instability modes. Nucl. Eng. Des. 95, 5–34.

Lahey, R.T., Drew, D.A., 1980. An assessment of the literature related to LWR instability modes. In: NUREG/CR-1414.

Lahey, R.T., Moody, F.J., 1977. The Thermal hydraulics of a Boiling Water Nuclear Reactor. ANS Monograph.

Peng, S., Podowsky, M., Lahey, R.T., 1986. BWR Linear stability analysis. Nucl. Eng. Des. 93, 25–37.

Rizwan-Uddin, 1994. On density-wave oscillations in two-phase flows. Int. J. Multiphase Flow 20, 721–737.

Rizwan-Uddin, Dorning, J.J., 1988. A chaotic attractor in a periodically forced two-phase flow system. Nucl. Sci. Eng. 100, 393–404.

Taleyarkhan, R., Podowski, M., Lahey, R.T., 1983. The development of a nodal method for the stability analysis of ventilated boiling channels. In: The Second International Topical Meeting on Nuclear Reactor Thermal Hydraulics, Sta. Barbara, CA, USA.

Xiao, M., Chen, X., Zhang, M., Veziroglu, T., Kakac, S., 1993. A multivariable linear investigation of two-phase flow instabilities in parallel boiling channels under high pressure. Int. J. Multiphase Flow 19, 65–77.